

## Conduction Threshold and Pinning Frequency of Magnetically Induced Wigner Solid

F. I. B. Williams,<sup>(1)</sup> P. A. Wright,<sup>(2)</sup> R. G. Clark,<sup>(2)</sup> E. Y. Andrei,<sup>(3)</sup> G. Deville,<sup>(1)</sup> D. C. Glattli,<sup>(1)</sup>  
O. Probst,<sup>(1)</sup> B. Etienne,<sup>(4)</sup> C. Dorin,<sup>(4)</sup> C. T. Foxon,<sup>(5)</sup> and J. J. Harris<sup>(5)</sup>

<sup>(1)</sup>*Service de Physique du Solide et de Résonance Magnétique Centre d'Etudes Nucléaires, Saclay, 91191 Gif-sur-Yvette, France*

<sup>(2)</sup>*Clarendon Laboratory, University of Oxford, Oxford OX1 3PU, United Kingdom*

<sup>(3)</sup>*Department of Physics, Rutgers University, Piscataway, New Jersey 08855*

<sup>(4)</sup>*Laboratoire de Microstructures et de Microélectronique, Centre National de la Recherche Scientifique, 92220 Bagneux, France*

<sup>(5)</sup>*Philips Research Laboratories, Redhill, Surrey RH1 5HA, United Kingdom*

(Received 14 September 1990)

The 2D quantum system of electrons at a GaAs/GaAlAs heterojunction in high magnetic field at low temperature is shown to exhibit conduction typical of pinned charge-density waves. Crossover from Ohmic conduction occurs on the same boundary at which radio-frequency resonances signal the onset of transverse elasticity. A further small non-Ohmic region is isolated from the main area by a  $\nu = \frac{1}{5}$  quantum-Hall-effect phase. The relationship found between the threshold conduction field and the resonance frequency is well accounted for by a model of a pinned electron crystal.

PACS numbers: 73.40.Kp, 64.70.Dv, 71.45.Lr, 73.20.Mf

Wigner predicted that upon lowering the density of an ideal quantum electron liquid it should crystallize because quantum fluctuation effects diminish more rapidly than Coulomb correlation. Real systems are also subjected to static fluctuations from the environment which must then be kept small with respect to the Coulomb interaction. This requirement puts a lower bound on the density for a given degree of perfection. The best realization to date is the two-dimensional (2D) electron system at modulation-doped GaAs/GaAlAs heterojunctions where this bound is  $\sim 100$  times the Wigner critical density. The cost of quantum fluctuations can be reduced by confining the zero-point motion to cyclotron orbits by means of a perpendicular magnetic field  $B$ . Then, as the orbit width  $l_c = (\hbar c/eB)^{1/2}$  approaches the mean interelectron distance, Coulomb correlation becomes important, leading first to fractional-quantum-Hall-effect (FQHE) states and ultimately to crystalline ordering of the orbit centers. Minimal conditions are that the temperature be lower than the classical melting temperature  $T_{mc}$ ,<sup>1</sup> and that the field be higher than that required for some critical Landau-level filling factor  $\nu = \nu_c \ll 1$ .<sup>1</sup> In fact, in the high-density limit, the state of the system should be a function of only the reduced variables  $t = T/T_{mc}$  and  $\nu$ . This provides a convenient test that a phenomenon is intrinsic. An extrinsic disorder field reduces electron order, first by breaking a crystal into domains and, if too strong, by destroying the  $(\nu, t)$  universality.

The solid differs from the liquid by its elastic response to shear, leading to transverse phonons and an inability to flow around obstacles. The liquid-solid transition was therefore identified by resonances in the radio-frequency (rf) absorption spectrum arising from magnetotransverse phonons<sup>2-5</sup> whose appearance gave a phase diagram

showing the above-mentioned universality (the  $t \rightarrow 0$  critical filling factor  $\nu_c = 0.192$ ), but whose frequencies were sample dependent. This latter feature was thought to arise from domain formation in the electron crystal. Another experiment<sup>6</sup> showed that conventional magnetoresistivity data could be fitted by an Arrhenius form with a characteristic temperature which shows a break in slope with field, taken to indicate  $\nu_c$ .<sup>7</sup> As for the flow properties of the new phase, hints of nonlinearity have only just been recognized.<sup>4,8</sup> The present experiments go beyond this work by demonstrating clearly that the new phase has a well-marked threshold in driving field, separating insulating from conducting behavior, which is quantitatively related to the magnetophonon spectrum. We show how an electron crystal pinned by a random field links the two types of observations.

The measurements were made on two modulation-doped heterojunctions: Sample I has a superlattice-protected buffer, a 160-nm undoped GaAlAs spacer, and a 200-nm volume-doped Si donor region,<sup>9</sup> while sample II, used in the simultaneous threshold and rf experiments, is double delta doped with a first spacer of 100 nm and a second one of 180 nm.<sup>10</sup>

Sample I was investigated both as-cooled and after preparation by brief illumination with a red light-emitting diode which increases its density  $n_s$  from  $\sim 4 \times 10^{10}$  to  $\sim 9 \times 10^{10} \text{ cm}^{-2}$ , its mobility from  $\sim 4 \times 10^6$  to  $\sim 9 \times 10^6 \text{ cm}^2 \text{ V}^{-1} \text{ s}^{-1}$  and greatly improves the contrast of the magnetoresistivity features (Fig. 1). These conventional four-point ac current-source measurements at  $T = 35 \text{ mK}$  ( $t = 0.07$ ) show deep minima in the diagonal resistivity  $\rho_{xx}$  at  $\nu = \frac{2}{9}$  and  $\frac{1}{5}$ , accompanied by plateaus in the Hall resistivity  $\rho_{xy}$ , on either side of an abnormally high maximum. The  $\rho_{xx}$  minima at  $\nu = \frac{2}{11}$  and  $\frac{1}{7}$  disappear above  $T = 50 \text{ mK}$  ( $t = 0.1$ ).

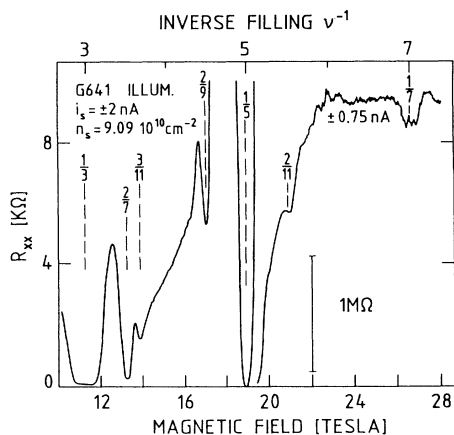


FIG. 1. Diagonal magnetoresistivity  $\rho_{xx}$  measured by a four-point, 7-Hz, current-source technique for sample I at 35 mK after illumination.

Flow response is contained in the current-voltage ( $I$ - $V$ ) characteristic, obtained by applying a slowly swept ( $> 200$  s) voltage  $U$  to one end of the sample and measuring the current  $i$  through the other; this avoids problems with very low conductances when using separate voltage probes. Because the Hall voltage and any contact threshold  $V_c$  reduce the potential drop, the observed  $i(U)$  is  $i = I(U - V_c - Ri)$ , where  $I(V)$  is the basic  $I$ - $V$  characteristic and  $R$  is the sum of the Hall, lead ( $\approx 50$  K $\Omega$ ), and differential contact resistances. By using current-biased contact pairs, we found corrections from  $V_c$  to be less than 1 mV. Threshold voltages  $V_T$  are derived by extrapolating  $i \rightarrow 0$  to eliminate  $Ri$ ; our protocol is to extrapolate the linear high- $U$  asymptote to the  $V$  axis, except where hysteresis and sometimes temporal current switching appears ( $\nu < \frac{2}{11}$ ,  $t < 0.15$ ), when we take  $V_T$  to be the lowest value at which a current jump occurs. Some data for sample I illuminated are shown in Fig. 2.

Threshold voltages are shown in Fig. 3. Extrapolation to vanishing threshold gives points in the  $(\nu, t)$  plane which map out the boundaries of three distinct regions,  $L$ ,  $S_1$ , and  $S_2$  (Fig. 4). The  $L$ - $S_1$  boundary, determined for two very different densities, is universal in  $(\nu, t)$  and coincides with the boundary determined from the appearance of rf resonances<sup>2-4</sup> (see also Fig. 5); the region  $S_2$ , sandwiched between  $\nu = \frac{2}{9}$  and  $\frac{1}{5}$ , was only clearly discernible for sample I illuminated.

The nonlinear  $I$ - $V$  characteristic approximates  $I(V) \propto \sinh(\text{const} \times V/T)$  for  $V \ll V_T$  [Fig. 2(c)], whose form is discussed below, and a linear form for  $V \gg V_T$ .<sup>11</sup> The ratio of differential resistances at  $V=0$  and at  $V > V_T$  can exceed  $10^4$  at low temperatures. This implies that if a FQHE liquid does coexist with the insulating phase, as the  $\nu = \frac{2}{11}$  and  $\frac{1}{7}$  dips of Fig. 1 might suggest, its concentration is insufficient for percolation. Figure 3 suggests that it may reflect instead an anomaly in the

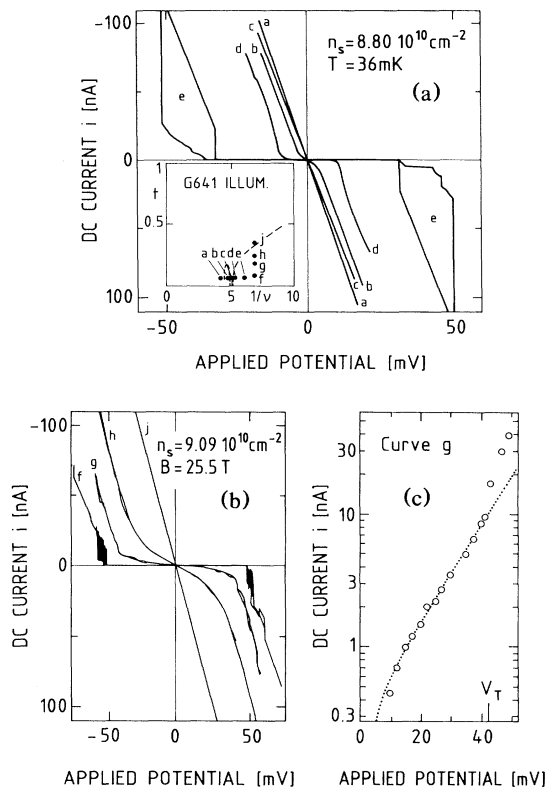


FIG. 2. (a)  $i(U)$  characteristic at  $T = 36 \pm 4$  mK and  $B = 15, 17.25, 18.2, 19.25,$  and  $22$  T for curves  $a, b, c, d,$  and  $e$ . (b)  $i(U)$  at  $B = 25.5$  T and  $T = 40, 104, 132,$  and  $192$  mK for curves  $f, g, h,$  and  $j$ . (c)  $\log(i)$  vs  $U$  for data labeled  $g$ . The dotted line is  $i = i_0 \sinh(N_D e E a / T)$  with  $N_D = 55$ ,  $E = U / (0.15$  cm) and  $T = 104$  mK. All data are for sample I illuminated. The reduced parameters  $(\nu, t)$  for each curve are identified in the inset. Hysteresis is visible for curve  $e$  and current switching for curve  $f$ .

threshold field. With such  $I$ - $V$  characteristics, care should be taken in interpreting usual  $R_{xx} = V(I)/I$  current-source transport data, for it becomes sensitive to source current.

A single-electron energy  $W_1 = eE_T a$  constructed from the measured threshold field  $E_T$  and  $a = (\pi n_s)^{-1/2}$  gives 1 mK for  $30$  mV cm<sup>-1</sup>: This threshold is visible at 100 mK, however, and so the effect must be collective. The sharp threshold, the hysteresis, and the switching phenomena are characteristic of pinned charge-density waves (CDW).<sup>12</sup> Like classic CDW systems, a 2D periodic configuration is unstable to domain formation in a random field.<sup>13</sup> In the weak-pinning limit, the energy gained by domains settling into potential fluctuations is opposed by their elastic strain, and the net pinning energy per domain is  $W_p \approx -\frac{1}{2} K a^2$ , where  $K$  is the shear modulus. These crystallite regions of average  $N_D$  electrons and size  $L_D$  can only be pulled away when the electric force per domain exceeds  $\approx K a$ , so the threshold

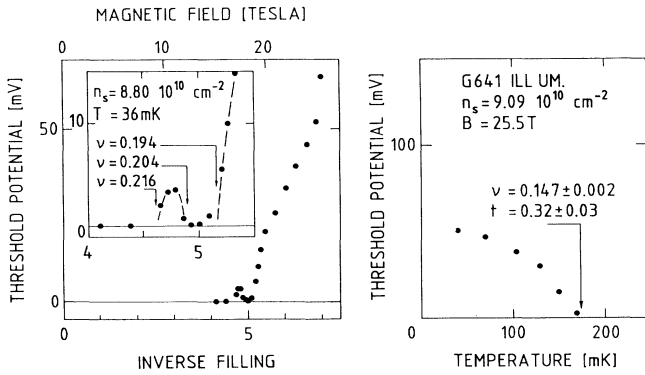


FIG. 3. Threshold potentials  $V_T$  for sample I illuminated extracted from curves as in Fig. 2. The field  $E_T = V_T / (0.15 \text{ cm})$ . The inset is an enlargement.

field affords an estimate for

$$N_D \approx Ka / eE_T \quad (1)$$

in which the proportionality factor is model dependent. For strong pinning, we expect a similar relation with a different factor on the grounds that in two dimensions, unlike one, the system can go around a strongly pinned electron by shearing bonds. Both  $K$  and  $N_D$  contribute to variation in  $E_T$ , but if we consider the upper bound to  $K$  to be its classical value, Eq. (1) gives  $N_D < 500$  for  $E_T = 250 \text{ mV cm}^{-1}$  (curve  $g$  in Fig. 2).

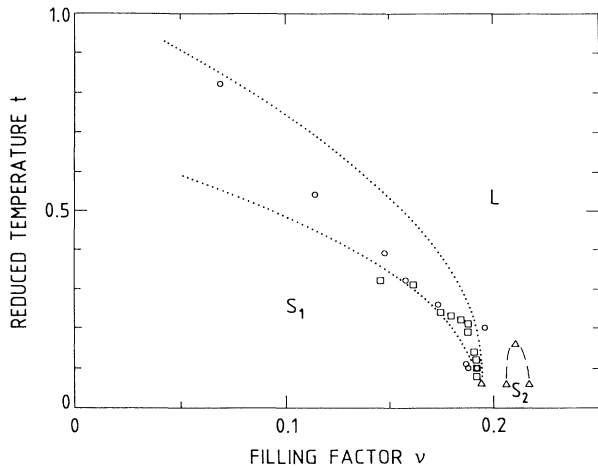


FIG. 4. Phase diagram in reduced variables  $(\nu, t)$  constructed from points  $(B, T)$  at which a conduction threshold appears. Open circles: as-cooled sample I,  $n_s = 3.8 \times 10^{10} \text{ cm}^{-2}$ ; open squares and triangles: sample I after illumination,  $n_s = 9 \times 10^{10} \text{ cm}^{-2}$ . Dotted lines indicate limits of scatter for the appearance of magnetophonon resonances in previous experiments (Refs. 2-4) using a wide variety of samples with  $3.5 \times 10^{10} < n_s < 12 \times 10^{10} \text{ cm}^{-2}$ . Dashed lines are guides to the eye. The  $L$ - $S_1$  boundary extrapolates to  $\nu_c = 0.193 \pm 0.003$  ( $t \rightarrow 0$ ) and  $t_c = 0.85 \pm 0.2$  ( $\nu \rightarrow 0$ ).

In the framework of a naive CDW-inspired “wash-board” model, domain motion is represented by a mass  $N_D m^*$  ( $m^*$  is electron effective mass) of charge  $N_D e$  in a sinusoidal electron lattice-periodic potential of amplitude  $N_D e E_T a / \pi$  in driving field  $E$ . In this model, independent domain motion would produce a current

$$I(E) \propto \sinh(N_D e E a / T) \exp - (2 N_D e E_T a / \pi T)$$

for  $E \ll E_T$ . This form fits the experiments quite well [Fig. 2(c)] with  $50 < N_D < 100$ .<sup>14</sup>

The pinning creates a restoring force with respect to the host milieu. This gives rise to a local mode<sup>15</sup> of shear origin which introduces a gap into the nominally gapless phonon excitation branch. In the absence of mode coupling by the Lorentz force, this pinning gap would have a frequency  $f_g$  characteristic of a shear mode of domain-size wavelength, expressible directly in terms of  $E_T$  by Eq. (1):

$$f_g \approx (K / n_s m^*)^{1/2} / 2L_D \approx (e E_T / 4 a m^*)^{1/2}. \quad (2)$$

The magnetophonon frequency  $f_-$ , still proportional to the shear modulus, now involves both the exciting field wavelength  $\lambda$  and the domain size  $L_D$ : If  $\lambda \gg L_D$ , the shear response is probed on the length scale set by the domains and the transverse frequency  $f_t(\lambda) \rightarrow f_g$ . However, the compressional response is dominated by the

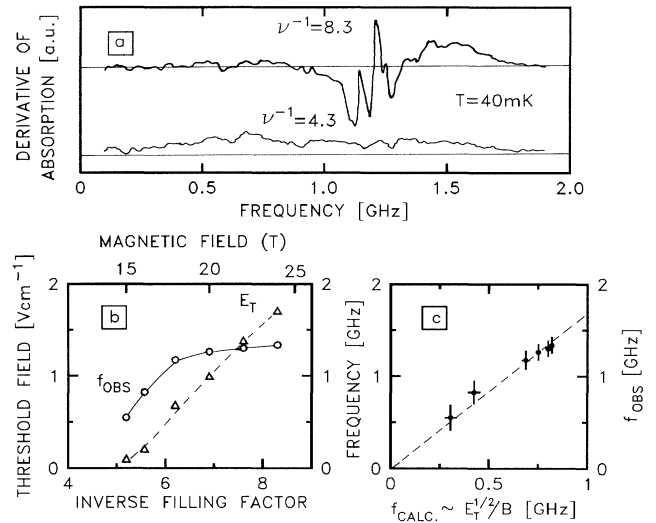


FIG. 5. (a) Examples of electron absorption spectra in regions  $L$  and  $S_1$  from a  $16\text{-}\mu\text{m}$  periodicity rf field. The sharp modulating structure is instrumental. (b) Observed frequency  $f_{\text{obs}}$  (open circles) of the lowest absorption line and simultaneously measured conduction threshold field  $E_T$  (open triangles) vs magnetic field  $B$ . (c) Observed frequency compared to that calculated from  $E_T$  and  $B$  using Eq. (3). Observations on sample II at  $T = 40 \text{ mK}$ ,  $n_s = 7.0 \times 10^{10} \text{ cm}^{-2}$  and mobility  $\approx 10^6 \text{ cm}^2 \text{ V}^{-1} \text{ s}^{-1}$ .

long-range Coulomb force and the longitudinal frequency  $f_l(\lambda) \rightarrow f_{pl}(\lambda) = (n_s e^2 / \epsilon m^* \lambda)^{1/2}$  of free plasmons. Consequently,

$$f_- = f_l(\lambda) f_l(\lambda) / f_c \approx f_g f_{pl}(\lambda) / f_c \propto E^{1/2} / B, \quad (3)$$

where  $f_c = eB / 2\pi m^* c$  is the cyclotron frequency. Figure 5 shows how this expression, with  $\lambda$  equal to the basic period  $\lambda_0 = 16 \mu\text{m}$  of the exciting field, relates *simultaneously* measured values of the resonance frequency  $f_{\text{obs}}$  to the threshold field  $E_T$  for sample II. The functional dependence  $f_{\text{obs}} \propto E_T^{1/2} / B$  holds over a factor of 20 in  $E_T$ ; the proportionality factor differs by  $\sim 40\%$ , but better agreement would be fortuitous for such estimates. We must now understand an isolated, "singlet," absorption<sup>3,4</sup> as the first of a series of wider spacing arising from a larger gap  $f_g$ . Indeed, the as-cooled type-I sample showing a 1.7-GHz singlet<sup>4</sup> revealed another line at 2.45 GHz and illumination transformed this spectrum into a narrow line multiplet at lower frequency.<sup>16</sup>

The sharpness of the conduction threshold, the universality in reduced variables  $(v, t)$  of its onset point, common with the appearance of the magnetophonon spectrum, as well as the quantitative relation between the two measurements can all be understood in terms of a pinned electron crystal.

We thank the CNRS-Max-Planck-Institut High Magnetic Field Laboratory in Grenoble; J. C. Picoche, C. Warth, P. Sala and most especially J. C. Vallier. C. Chaleil and J. Verrier made essential technical contributions. Partial support was provided by NSF grant No. DMR87-05-977 and a NATO travel grant. R.G.C. and P.A.W. thank the Science and Engineering Council, United Kingdom, for financial support.

<sup>1</sup> $T_{mc} = e^2 / \epsilon a \Gamma_m$ , where  $\Gamma_m = 127$ ,  $\epsilon = 13$ , and  $a = (\pi n_s)^{-1/2}$ . Filling factor  $\nu = n_s hc / eB = 2l_c^2 / a^2$  (cgs Gaussian units).

<sup>2</sup>E. Y. Andrei, G. Deville, D. C. Glattli, F. I. B. Williams, E.

Paris, and B. Etienne, Phys. Rev. Lett. **60**, 2765 (1988).

<sup>3</sup>D. C. Glattli, G. Deville, V. Duburcq, F. I. B. Williams, E. Paris, B. Etienne, and E. Andrei, Surf. Sci. **229**, 344 (1990).

<sup>4</sup>F. I. B. Williams, E. Y. Andrei, R. G. Clark, G. Deville, B. Etienne, C. T. Foxon, D. C. Glattli, E. Paris, and P. A. Wright, in *Localization and Confinement of Electrons in Semiconductors* (Springer-Verlag, Berlin, 1990), p. 192.

<sup>5</sup>H. L. Stormer and R. L. Willett, Phys. Rev. Lett. **62**, 972 (1989); E. Y. Andrei, G. Deville, D. C. Glattli, F. I. B. Williams, E. Paris, and E. Etienne, Phys. Rev. Lett. **62**, 1926 (1989) (corrected Reply).

<sup>6</sup>R. L. Willett, H. L. Stormer, D. C. Tsui, L. N. Pfeiffer, K. W. West, and K. W. Baldwin, Phys. Rev. B **38**, 7881 (1988).

<sup>7</sup>H. W. Jiang, R. L. Willett, H. L. Stormer, D. C. Tsui, L. N. Pfeiffer, and K. W. West, Phys. Rev. Lett. **65**, 633 (1990).

<sup>8</sup>V. J. Goldman, J. E. Cunningham, M. Shayegan, and M. Santos, Phys. Rev. Lett. **65**, 2188 (1990).

<sup>9</sup>C. T. Foxon, J. J. Harris, D. Hilton, J. Hewett, and C. Roberts, Semicond. Sci. Technol. **4**, 582 (1989).

<sup>10</sup>B. Etienne and E. Paris, J. Phys. (Paris) **48**, 2049 (1987).

<sup>11</sup>Reference 8 reports contrary behavior: Ohmicity for low driving fields and slight nonlinearity above threshold. Only data very near the phase boundary are shown in Ref. 8, but the extent of the plateaus in differential impedance is roughly in line with our threshold-field plot in Fig. 3. This Ohmic plateau disappeared on essentially the same phase boundary as reported here and previously (Refs. 2-4).

<sup>12</sup>See the review by G. Grüner and A. Zettl, Phys. Rep. **119**, 117 (1985).

<sup>13</sup>Y. Imry and S. Ma, Phys. Rev. Lett. **35**, 399 (1975).

<sup>14</sup>It is of possible relevance to the Arrhenius fits of Refs. 6-8 that in the low- $E$  limit,  $R \propto E/I \propto T \exp(cE_T/T)$ . Experimentally,  $E_T = b(T_m - T)$ , from which  $R \propto T \exp(cbT_m/T)$ , so the characteristic temperature may not be fundamental, the constants  $c$  and  $b$  being sample dependent. Nonetheless, it vanishes at  $\nu = \nu_c$ , inasmuch as  $T_m(\nu_c) = 0$ .

<sup>15</sup>H. Fukuyama and P. A. Lee, Phys. Rev. B **17**, 535 (1978).

<sup>16</sup>D. C. Glattli *et al.*, Physica (Amsterdam) **169B**, 328 (1991). Equation (3) would describe the multiplet of Ref. 2 as a harmonic sequence  $\lambda = \lambda_0/p$  ( $p = 1, \dots, 5$ ) with  $f_{pl}(\lambda) \propto p^{1/2}$  (unscreened plasmons) and  $f_g \approx 70$  GHz, implying  $N_D > 80$ .